



Hydroclimate variability of the northwestern Amazon Basin near the Andean foothills of Peru related to the South American Monsoon System during the last 1600 years

J. Apaéstegui^{1,3,4}, F. W. Cruz², A. Sifeddine^{3,4,12}, M. Vuille⁵, J. C. Espinoza^{1,6}, J. L. Guyot⁸, M. Khodri^{3,7}, N. Strikis², R. V. Santos⁹, H. Cheng^{10,11}, L. Edwards¹¹, E. Carvalho⁹, and W. Santini⁸

¹Instituto Geofísico del Peru, Lima, Peru

²Instituto de Geociências, Universidade de São Paulo, São Paulo, Brazil

³LMI “PALEOTRACES” (URD/UFF/Uantof-Chili), Departamento de Geoquímica-UFF, [TSL](#), Brazil

⁴Departamento de Geoquímica, Universidade Federal Fluminense, Niterói-RJ, Brazil

⁵University of Albany, SUNY, Albany, NY, USA

⁶Universidad Agraria La Molina, Lima, Peru

⁷UMR LOCEAN (IRD/UPMC/CNRS/MNHN), Paris-Jussieu, France

⁸UMR GET (IRD) Géosciences Environnement Toulouse, CNRS-IRD-UPS, OMP, Toulouse, France

⁹Instituto de Geociências, Universidade de Brasília, Brasília, DF, Brazil

¹⁰Institute of Global Environmental Change, Xi’an Jiaotong University, Xi’an, China

¹¹Department of Geology and Geophysics, University of Minnesota, Twin Cities, Minneapolis, Minnesota, USA

¹²LOCEAN (CNRS, IRD, MNHN, UPMC), Bondy, France

Correspondence to: J. Apaéstegui (japaestegui@gmail.com)

Received: 3 January 2014 – Published in Clim. Past Discuss.: 10 February 2014

Revised: 9 October 2014 – Accepted: 13 October 2014 – Published:

Abstract. In this paper we explore a speleothem $\delta^{18}\text{O}$ record from Palestina cave, northwestern Peru, at a site on the eastern side of the Andes cordillera, in the upper Amazon Basin. The $\delta^{18}\text{O}$ record is interpreted as a proxy for South American Summer Monsoon (SASM) intensity and allows the reconstruction of its variability during the last 1600 years. Two periods of anomalous changes in the climate mean state corresponding to the Medieval Climate Anomaly (MCA) and the Little Ice Age (LIA) periods identified in the Northern Hemisphere are recognized in the record, in which decreased and increased SASM activity, respectively, have been documented. Variations in SASM activity between the MCA and the LIA seem to be larger over the northern part of the continent, suggesting a latitudinal dependence of the MCA footprint. Our results, based on time series, composite and wavelet analyses, suggest that the Atlantic Multidecadal Oscillation (AMO) plays a relevant role for SASM modulation on multidecadal scales (~ 65 years), especially during dry periods such as the MCA. Composite analyses, applied

to evaluate the influence of the AMO on the Palestina cave $\delta^{18}\text{O}$ and other $\delta^{18}\text{O}$ -derived SASM reconstructions, allow insight into the spatial footprints of the AMO over tropical South America and highlight differences between records during key studied periods. This work also reveals that replicating regional climate signals from different sites, and using different proxies is absolutely essential for a comprehensive understanding of past changes in SASM activity.

1 Introduction

South American paleoclimate reconstructions over the last millennium based on $\delta^{18}\text{O}$ from different proxies such as speleothems, lake sediments and ice cores have shown regionally coherent patterns of change during distinct events recognized as the Medieval Climate Anomaly (MCA; AD 900–1250) and the Little Ice Age (LIA; AD 1400–1850) (e.g., Thompson et al., 1986, 2013; Rabatel et al., 2008;

Reuter et al., 2009; Jomelli et al., 2009; Bird et al., 2011a; Vuille et al., 2012; Novello et al., 2012; Kanner et al., 2013). These climate anomalies are primarily manifested as changes in temperature over Northern Hemisphere oceanic and continental areas but appear more strongly related to variations in hydroclimatic conditions over tropical South America (e.g., Bird et al., 2011a; Vuille et al., 2012). Both the LIA and the MCA have been identified in documentary and proxy records from the Northern Hemisphere where warm/dry conditions were inferred from several proxies during the MCA (e.g., Graham et al., 2010 and references cited therein) while cold/wet conditions have been inferred from glaciers advancing through the LIA period (e.g., Mann et al., 2002 and references cited therein).

In the South American Andes, one of the first climate reconstructions for the last 1500 years was produced in the 1980s based on the oxygen isotopic signal ($\delta^{18}\text{O}$) from the Quelccaya ice core (Thompson et al., 1986). The LIA was recognized in this record as a period with more negative values of ice $\delta^{18}\text{O}$, originally interpreted as reflecting cold periods. Other studies based on speleothem $\delta^{18}\text{O}$ records from the eastern Andes suggested that rainfall during the LIA increased by approximately 20% compared to the 20th century (Reuter et al., 2009). Moreover, a recently published study based on authigenic calcite $\delta^{18}\text{O}$ deposited in annually laminated lacustrine sediments of a high-altitude lake on the eastern flank of the Andes postulated an intensification of the South American Summer Monsoon (SASM) during the LIA period and diminished SASM activity during the MCA interval (Bird et al., 2011a). The climatic controls on the $\delta^{18}\text{O}$ signal in Andean ice core records are considered to be the same as those proposed from the carbonate records from speleothems and lake records within the SASM domain (Vuille et al., 2012) because all these records primarily reflect the isotopic composition of monsoonal rainfall (Vuille and Werner, 2005; Vimeux et al., 2005). However, the actual regional-scale response to changes in radiative forcing during the MCA and LIA is still poorly understood due to the lack of sufficient highly resolved and chronologically well-constrained isotopic proxy records from the region. For example, it remains unclear how changes in rainfall partitioning between the Amazon lowlands and the Andean high-elevation sites may have affected the isotopic response (e.g., Bird et al., 2011b). Previous studies have also detected differences in the timing of MCA and LIA in tropical South America (Bird et al., 2011a; Vuille et al., 2012), but it is debatable to what extent these offsets are real or related to chronological errors. Several studies have also pointed toward a distinct antiphased regional rainfall response during the LIA, with increased precipitation over the tropical Andes and southern Brazil (Oliveira et al., 2009; Vuille et al., 2012), while drier conditions were recorded over northeastern Brazil (Novello et al., 2012). Similarly a relatively dry climate is documented during the MCA over the Andes and in NE Brazil, while

southern Brazil speleothems do not clearly document this dry period.

Aside from the lack of records to adequately map the regional climate response to the perturbed climate states during the LIA and MCA when compared to the Current Warm Period (CWP; Bird et al., 2011a), the dynamical mechanisms involved in changing the SASM mean state and its spatial footprint are still not fully understood. Recent studies suggest that teleconnections between the Pacific and Atlantic oceans affect SASM intensity and/or rainfall distribution over South America at different timescales (e.g., Kanner et al., 2013; Novello et al., 2012). How these modes of variability and their interactions change in response to changes in radiative forcing is of major importance for understanding past and future SASM variations. In fact, there is considerable concern that the SASM dynamics will be significantly affected by increasing greenhouse gas concentrations in the 21st century (Seth et al., 2010). Hence, there is an urgent need to better document and understand the causes of monsoon variations in response to natural forcing during the most recent past (Vuille et al., 2012). Yet modeling studies, which could help diagnose past changes in SASM dynamics, still suffer greatly from a lack of proxy data to validate their simulations.

Here we explore new high-resolution $\delta^{18}\text{O}$ records of well-dated speleothems PAL3 and PAL4 collected in Palestina cave on the eastern side of the Andes Cordillera (northeastern Peru) and discuss them in the light of existing paleoclimate proxies along the Andes, which have similarly been interpreted as recording the intensity of the SASM. The Palestina records span the last millennium with ~ 5 -year temporal resolution, allowing us to explore the SASM variability as recorded at this site from sub-decadal to centennial time-scales. Time series and wavelet analyses are performed in order to identify oceanic and atmospheric modes and their teleconnections affecting past SASM activity. Additionally, composite techniques are applied to explore possible mechanisms that could explain the observed spatiotemporal SASM variability across the tropical South American continent over the past 1600 years.

2 Study area and modern climatology

The Palestina cave (Nueva Cajamarca, San Martín, Peru) was explored over a length of 2380 m by the Bristol Exploration Club (BEC, UK) in 2003, and mapped by the French–Peruvian GSBM–ECA team in 2011. The cave is located in northeastern Peru (5.92°S , 77.35°W), in the upper Amazon Basin along the eastern margin of the Andes (870 m a.s.l.) in a Triassic–Jurassic limestone–dolomitic formation (INGEMET-Peru; Fig. 1). The present-day climate is tropical humid with a mean annual temperature of 22.8°C , and mean annual precipitation around 1570 mm, measured ~ 15 km from the cave, in the meteorological station of Ri-

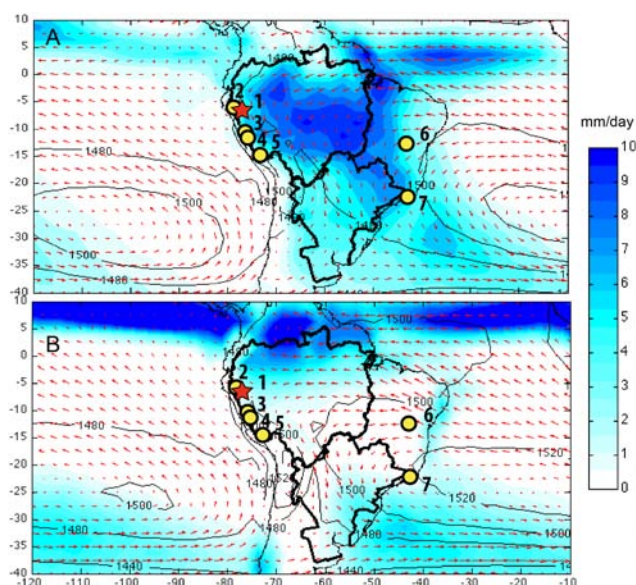


Figure 1. Geopotential height (contours, in geopotential meters – gpm) and total wind at 850 hPa from ERA-40 for the 1975–2002 period and mean daily rainfall from CMAP data for the 1979–2002 period. Panel (a) shows during DJF season; (b) during JJA season. Limits of the Amazon Basin are shown. The numbers in the figure indicate locations of other proxy records in South America. Point (1) Palestina record (this study); (2) Cascayunga cave record (Reuter et al., 2009); (3) Pumacocha lake record (Bird et al., 2011a); (4) Huagapo cave record (Kanner et al., 2013); (5) Quelccaya Ice Cap (Thompson et al., 1986); (6) DV2 cave record (Novello et al., 2012); (7) Cristal cave Record (Taylor, 2010).

oja during the period 1963–2012. Rainfall displays a bimodal distribution featuring a rainy season between October and March, which represents around 63 % of the total annual rainfall. A tropical circulation regime allowing precipitation during the winter and early spring (April–September) is responsible for the remaining 37 % of total rainfall. This precipitation regime results from the seasonal march of convective activity over the tropical continent associated with the onset, mature phase and demise of the SASM (Marengo and Nobre, 2001; Espinoza et al., 2009; Garreaud et al., 2009).

On interannual timescales, changes in SASM intensity are partially related to sea surface temperature (SST) anomalies in the tropical Pacific associated with El Niño–Southern Oscillation (ENSO) (Nogués-Paegle and Mo, 2002; Garreaud et al., 2009; Grimm, 2010 and references cited therein). During the warm or positive phase of ENSO (El Niño), below average precipitation during the summer wet season is observed in northern South America, especially over the northeast of the Amazon Basin (Ronchail et al., 2002), the tropical Andes (Garreaud et al., 2003) and occasionally in the western Amazon (Espinoza et al., 2011). The opposite conditions are observed during cold or negative phases (La Niña), where abundant rainfall and flooding occurs in the north and north-

east of the Amazon region (Ronchail et al., 2002; Espinoza et al., 2009, 2013) as a result of adjustments in the location and strength of the Walker and Hadley circulations to the underlying Pacific sea surface temperature anomalies (SSTA; Ronchail et al., 2002; Garreaud et al., 2009; Marengo et al., 2012). The influence of Atlantic SSTA on the interannual variability of the SASM has not been studied in similar detail as the influence of Pacific SSTA. Warm SSTA in the tropical North Atlantic region have been associated with drought conditions over the southern (e.g., Yoon and Zeng, 2010; Ronchail et al., 2002; Marengo et al., 2008) and western Amazon Basin (Espinoza et al., 2011; Lavado et al., 2012). For instance, the 2005 and 2010 droughts over Amazonia were not related to ENSO but to anomalously warm SST in the tropical North Atlantic (Espinoza et al., 2011; Marengo et al., 2008, 2012).

On decadal and longer timescales SASM activity is less well understood, mainly because of limitations in the instrumental data. The Pacific Decadal Oscillation (PDO) is considered an important modulator of South American precipitation, with a very similar, albeit slightly weaker, spatial footprint over South America as ENSO, and with teleconnection mechanisms that are also similar to those observed for ENSO on interannual timescales (Garreaud et al., 2009). Linkages to the Atlantic Multidecadal Oscillation (AMO), with periodicities of ~ 64 years have also been documented as an important factor driving SASM variability, based on evidence from continental proxy records (Novello et al., 2012), marine sediments (Chiessi et al., 2009) and model simulations (e.g., Parsons et al., 2014). Yet previous paleoclimatic studies performed at high and lowland sites in the Andes (e.g., Reuter et al., 2009; Bird et al., 2011 [TS2](#)) did not perform statistical analyses of the stable isotope data to confirm the presence of decadal to multidecadal changes in monsoon intensity. Thus, there is still virtually no information available on the climate response to multidecadal forcing over the Amazon region.

Oxygen isotopes ($\delta^{18}\text{O}$) in rainfall over South America suggest that fractionation processes are to some extent related to the amount effect (between -0.4 and -0.8 ‰ per 100 mm increase in the mean annual precipitation; Reuter et al., 2009). Moreover, recent studies based on isotope-enabled numerical models demonstrate that the degree of moisture recycling and rainout upstream over the Amazon Basin associated with the intensity of the SASM is a significant first-order controlling factor (Vuille and Werner, 2005; Vuille et al., 2012; Kanner et al., 2013). The SASM is considered to be the main contributor to seasonal rainfall in the study area (63 %), although precipitation related to residual equatorial rainfall during austral winter is still significant (37 %) and isotopically different from the SASM $\delta^{18}\text{O}$ signature.

3 Materials and methods

A monitoring program was setup between May 2011 and September 2013 in order to evaluate the isotopic signature of precipitation and cave seepage waters related to speleothem formation. Water samples for isotope analyses (15 mL bottles) were collected twice a month in the isotope rainfall collector installed close to the cave entrance, and also in the Palestina spring that forms the Jordan river (which forms Palestina cave). Additional samples from cave drip waters were taken for comparison with the calcite signature obtained from the speleothems collected. Unfortunately, logistical problems lead to a loss of most samples during year 1 of the monitoring program. Therefore data availability is sparse for 2011, but continuous for most of the variables during the period January 2012–October 2013. Water analyses were performed in the Laboratorio de Estudos Geodinâmicos e Ambientais at the University of Brasília (UnB) using a Picarro L2120-i water isotope analyzer which allows measurements at an analytical precision of 0.03 ‰ and reports to $\delta^{18}\text{O}$ ‰ relative to Vienna Standard Mean Ocean Water (SMOW) standard.

Two speleothems were collected in the Palestina cave at a distance of 600 and 700 m from the entrance and ~ 80 m below the surface. Stalagmites PAL3 and PAL4 are ~ 10 and ~ 17 cm tall. The stable isotope profiles presented in this study were obtained from the first 40 mm (PAL3) and 80 mm (PAL4) of these speleothems, respectively. The age model developed for PAL4 is constrained by 13 U–Th ages and the one for PAL3 by 6 U–Th ages. The U–Th analyses were performed at the Minnesota Isotope Laboratory, University of Minnesota, using an inductively coupled plasma mass spectrometry (ICP-MS) technique (Cheng et al., 2013). The chemical procedures used to separate uranium and thorium fractions for ^{230}Th dating are similar to those described by Edwards et al. (1987), where most dates present errors of $2\sigma < 1\%$, representing a mean value of ~ 15 years (Tables S1 and S2 in the Supplement). The chronological model was developed for each speleothem by linearly interpolating ages between dates.

Analyses of $\delta^{18}\text{O}$ were performed with a Finnigan Delta Plus Advantage (Thermo Fisher Scientific) mass spectrometer, in the Laboratorio de Estudos Geodinâmicos e Ambientais at the University of Brasília (UnB). For $\delta^{18}\text{O}$, error analyses were 0.1 ‰. Records are reported as $\delta^{18}\text{O}$ ‰ relative to the Vienna Pee Dee belemnite (PDB) standard. 264 samples were collected over a length of 8 cm, along the growth axis of PAL4 stalagmite, sampling at an interval of 0.3 mm, using a Sherline micro-drill model 5400, coupled to an automated XYZ Stage. This sampling approach provides a temporal resolution between 2 and 10 years (~ 5 years).

The oxygen isotope profile of PAL3 is based on 200 analyses using a 100 μm sampling interval for the first 16 mm using a micro-milling machine system with a high-speed precision drill and stereomicroscope with a charged coupled de-

vice, mounted for XYZ motion control, in order to obtain a high resolution for the most recent period recorded in the speleothem. Between 16 and 39 mm, a 0.3 mm sampling interval was used for comparison with $\delta^{18}\text{O}$ values of PAL4 samples. These samples were also analyzed in the Laboratório de Estudos Geodinâmicos e Ambientais at the University of Brasília (UnB) using a Kiel IV carbonate device coupled to a Finnigan MAT 253 mass spectrometer (Thermo Fisher Scientific). This device allows optimizing the sample mass for analyses ($\leq 20 \mu\text{g}$ of carbonate), and the analytical precision obtained is $\pm 0.06\%$ for $\delta^{13}\text{C}$ and $\pm 0.09\%$ for $\delta^{18}\text{O}$.

Spectral analysis techniques were performed on the annually interpolated composite record of PAL4 and PAL3 $\delta^{18}\text{O}$ time series. Wavelet analysis (Torrence and Compo, 1998) is used to display the frequency variability of the $\delta^{18}\text{O}$ time series, while cross-wavelet analysis (Grinsted et al., 2004) is used to test the similarity and coherence in periodicities between our $\delta^{18}\text{O}$ records and other reconstructed indices on multidecadal timescales. In order to quantify the AMO influence on South American paleo-records during the common period between AD 734 and 1922, $\delta^{18}\text{O}$ composites were created for both positive and negative phases of the AMO, using the 25th and 75th percentiles as thresholds to define the negative (AMO–) and positive (AMO+) phases, respectively. A Student's t test was employed to test whether departures in the $\delta^{18}\text{O}$ composites were significantly different from the long-term mean in each proxy. Regional maps for $\delta^{18}\text{O}$ during AMO+ and AMO– were created to assess whether spatial patterns emerge that would characterize the AMO influence on $\delta^{18}\text{O}$ records.

4 Results and discussion

4.1 Stable isotopic composition of precipitation and speleothems

The local meteorological water line (LMWL) obtained from 40 values of $\delta^{18}\text{O}$ and δD pairs from each rainfall sampled nearby Palestina cave has a slope of ~ 8.2 , which is very close to the global meteorological water line (GMWL; Rozanski et al., 1992; Fig. S3 in the Supplement). Rainwater samples exhibit a range of $\delta^{18}\text{O}$ from -0.61 to -15.12% and co-vary with seasonal changes in precipitation. Still, the amount effect does not explain the total variance in the isotopic composition of precipitation ($R^2 = 0.3$, $p < 0.01$). Additional influences, mostly related to the degree of rainfall upstream over the Amazon Basin, affect the isotopic signal (Bird et al., 2011a; Vuille et al., 2012; Kanner et al., 2013). During the austral summer season, a higher percentage of isotopically depleted air masses originating over the Atlantic Ocean and transported across the Amazon Basin reach the cave site. These more distal air masses have been affected by the loss of heavy isotopes during periods of strong convec-

tive activity over the core SASM region. During austral winter, on the other hand, enriched values of $\delta^{18}\text{O}$ characterize the residual tropical rainfall in association with diminished rainout upstream due to weaker convective activity.

Rainwater exhibits relatively large variations in comparison with river water (from -6.47 to -11.91 ‰, $n = 22$) and drip waters (from -5.42 to -7.42 ‰, $n = 7$). Speleothem calcite $\delta^{18}\text{O}$ presents mean values of -7.11 ‰ (PDB), which is consistent with mean values recorded for river water (-7.9 ‰, SMOW) and rain water (-6.73 ‰, SMOW). The limited range of values in the river and drip waters indicates attenuation of the seasonal isotopic variations in rainfall related to mixing during meteoric water recharge. This effect might be triggered by variations in the hydraulic head depending on rainfall intensity as suggested for extreme values in $\delta^{18}\text{O}$ from the river waters, which allows observations of variations in relation to rainfall events. In this sense, intense recharge during the humid monsoon season is what triggers the infiltration and drip inside the cave, and hence degassing and deposition of calcite inside the cave.

4.2 Description of the Palestina record

The PAL3 and PAL4 calcite speleothems present micro-crystalline fabric and no apparent “hiatus” was detected. The twenty U–Th dates in PAL4 and PAL3 reveal that samples cover the period from $\text{AD } 413 \pm 10$ to 1824 ± 16 years and from $\text{AD } 1096 \pm 15$ to 1925 ± 8 years, respectively. Mean growth rates for PAL4 and PAL3 are 0.056 and 0.049 mm yr^{-1} , respectively. Sampling spacing of 0.3 mm for PAL4 and 0.01 mm for PAL3 yields a data resolution between 2 and 8 years (~ 5 years) for both speleothems (Fig. 2). For the climate interpretation of spectral signals, however, we chose a conservative estimate and refrain from interpreting signals at frequencies below 16 years (twice the lowest resolution of the record).

Stable oxygen isotopes for the entire records in PAL4 and PAL3 stalagmites present absolute mean values of -7.14 and -7.08 ‰, respectively. These values are in agreement with other results obtained from speleothems in the same region (Van Breukelen et al., 2008; Reuter et al., 2009). Stable oxygen and carbon isotope ratios ($\delta^{18}\text{O}$ and $\delta^{13}\text{C}$) are poorly correlated along the growth axis for both speleothems (PAL4, $R^2 = 0.26$, $n = 252$ and PAL3, $R^2 = 0.01$, $n = 195$, Fig. S4), which indicates that calcite deposition occurred close to equilibrium conditions with drip water (Hendy, 1971^{TS3}). Further tests to rule out kinetic fractionation were not carried out due to the difficulty of extracting samples from exactly the same layer. Moreover, even though the speleothems have different sampling resolutions and age models, the two oxygen isotope records are nearly identical both in terms of the mean values and the magnitude of change through the overlapping ~ 900 -year interval (Fig. 2). These similarities suggest that a common factor governs the isotopic signal in both speleothems,

and in the water infiltrating the cave environment, most likely related to SASM precipitation.

A composite oxygen isotope ($\delta^{18}\text{O}$) time series was created from the PAL4 and PAL3 records (Fig. 3a). The composite $\delta^{18}\text{O}$ record, hereafter referred to as the Palestina record, indicates major changes in the oxygen isotope ratio over different periods. Heavier values of $\delta^{18}\text{O}$ are recorded between $\text{AD } 421\text{--}580$, $722\text{--}820$ and during the MCA ($\text{AD } 920\text{--}100$) which is marked by a double peak of enriched $\delta^{18}\text{O}$ values centered at $\text{AD } \sim 940$ (~ -6.3 ‰) and at $\text{AD } \sim 1025$ (~ -5.8 ‰). Lighter or more negative values are observed between $\text{AD } 580\text{--}720$, $820\text{--}920$ and during the period $1325\text{--}1820$, which corresponds to the Little Ice Age in the Palestina record. The LIA period is characterized by a gradual but substantial decrease in $\delta^{18}\text{O}$ values with minimum values observed between $\text{AD } 1400$ and 1593 (-7.6 ‰; Fig. 3a), after which values increase gradually toward $\text{AD } 1820$, representing the end of the LIA in the Palestina record.

Spectral analysis of our record indicates significant periodicities centered on 70, 44 and 29 years, within 95 % statistical confidence (Fig. S5). Wavelet analyses support these results, indicating statistically significant superimposed periodicities (Fig. S6). During most of the MCA low-frequency variability dominates, centered at ~ 70 and 48 years. During the LIA, decadal variability (~ 10 years) appears to be more significant and persistent.

4.3 Comparison with other regional isotopic proxies

A comparison between the Palestina cave isotope record and other high-resolution proxies of SASM activity in the Andes is shown in Fig. 3. There is a striking resemblance between the Palestina and Pumacocha lake records at decadal to centennial timescales (Bird et al., 2011a) throughout most of the record (Figs. 3c and S7), confirming the regional-scale nature of the $\delta^{18}\text{O}$ signal and that the mean state changes of the SASM during the MCA and LIA periods also affected Palestina cave. Between $\text{AD } 430$ and 900 , however, the Palestina cave isotope record differs from the Pumacocha record. Afterwards similarities between the two records become more evident, suggesting a stronger regional control of the SASM during the past millennium. Interestingly, two distinctive decadal-scale peaks of more positive values centered at $\text{AD } \sim 940$ and ~ 1020 are recorded in both proxies during the MCA. Furthermore, a gradual decrease of $\delta^{18}\text{O}$ values starting at $\text{AD } \sim 1325$ can be identified in both records, but whereas minimum values are observed between $\text{AD } 1480$ and 1600 in the Palestina record, they occur more than a hundred years later in the Pumacocha record. Nonetheless, the Palestina record confirms many characteristic climatic features from the past millennium first detected in the Pumacocha record, which is quite remarkable given the different origin of the calcite (speleothem vs. lake sediments) obtained from very different Andean environments (lowlands

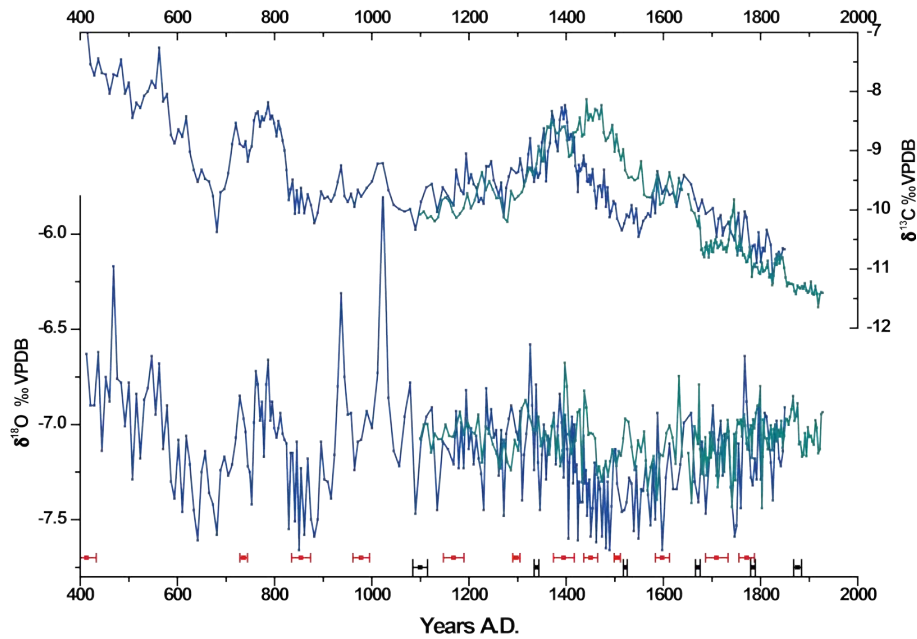


Figure 2. Stable isotope time series of $\delta^{13}\text{C}$ and $\delta^{18}\text{O}$ for PAL4 (blue line) and PAL3 (cyan line), respectively. U–Th dates and corresponding error bars are represented by red and black dots for PAL4 and PAL3 stalagmites, respectively.

vs. high Andes), ~ 500 km away and 3400 m elevation difference. The fact that the Palestina record shows evidence of many of the same features detected in Pumacocha (e.g., the double-peak structure of the MCA), highlights the value of data replication and of establishing dense regional proxy networks. Only by replicating such signals with independent records can they unambiguously be attributed to climate forcing as opposed to non-climatic effects.

Other records based on speleothems of the Andean region are represented by $\delta^{18}\text{O}$ series from the Cascayunga and Huagapo caves. Comparison with the Cascayunga speleothem record (Reuter et al., 2009; Fig. 3b), which is located close to Palestina cave (~ 20 km away), shows generally similar variations in $\delta^{18}\text{O}$ during the last 900 years. Two periods of heavier $\delta^{18}\text{O}$ values stand out in the Cascayunga record: AD 1278–1320 and 1485–1570. These features are to some extent also apparent in the Palestina record; especially the latter period, which is less evident in all other Andean $\delta^{18}\text{O}$ reconstructions. Nevertheless, these features are shared with a T/P index of upslope convective activity based on the ratio between cloud transported pollen from the Andean forest to the bog (T) and Poaceae pollen frequencies, related to the edaphic moisture of the Paramo (P) record obtained from Papallacta in the Andes of Ecuador (Ledru et al., 2013^{TS4}). It should be noted however, that the Cascayunga record lacks chronological control between ~ 1090 and 1450. If the $\delta^{18}\text{O}$ record from Cascayunga is adjusted within the age uncertainties as suggested in Fig. 3b, the discrepancies between proxies could at least partially be resolved. Unfortunately, the Cascayunga record does not extend back far enough to allow

a comparison with the variations observed by the Palestina record at the beginning of the last millennium.

When compared with the Huagapo cave record (Fig. 3d), an anti-phased relationship can be observed between AD 400 and 900. The Huagapo cave record also does not show an abrupt migration to heavier values during the MCA as is observed during the period AD 900–1100 in the Palestina and Pumacocha records. Afterwards, the $\delta^{18}\text{O}$ values at Huagapo cave gradually decrease between AD 1365 and 1820, which is in agreement with the LIA period in the Palestina record. The onset of the gradual decrease in $\delta^{18}\text{O}$ at Huagapo is delayed by ~ 40 years when compared with Palestina and Pumacocha, but this time frame is close to chronological uncertainty. However, the LIA period, defined in the Huagapo record as between AD 1450 and 1850 (Kanner et al., 2013), is shorter than for the other records in the Andean region presented earlier.

The Quelccaya ice core (Thompson et al., 1986; Fig. 3e) also shows similar variations in the mean state of the SASM during the past 1500 years. This record also confirms the regional coherence in the $\delta^{18}\text{O}$ signal along the Andes; however, there are several offsets in the timing of key periods such as the MCA and LIA. Recent definitions of the MCA (AD 1100–1300) and LIA (early LIA 1520–1680, late LIA 1681–1880) events in the Quelccaya record (Thompson et al., 2013) differ from the timing of these events as detected in carbonate records presented above. Moreover, a double peak of heavier $\delta^{18}\text{O}$ values is observed at AD 990 and 1080, which might be related to the double peak observed in the Palestina and Pumacocha records. Centennial-scale variabil-

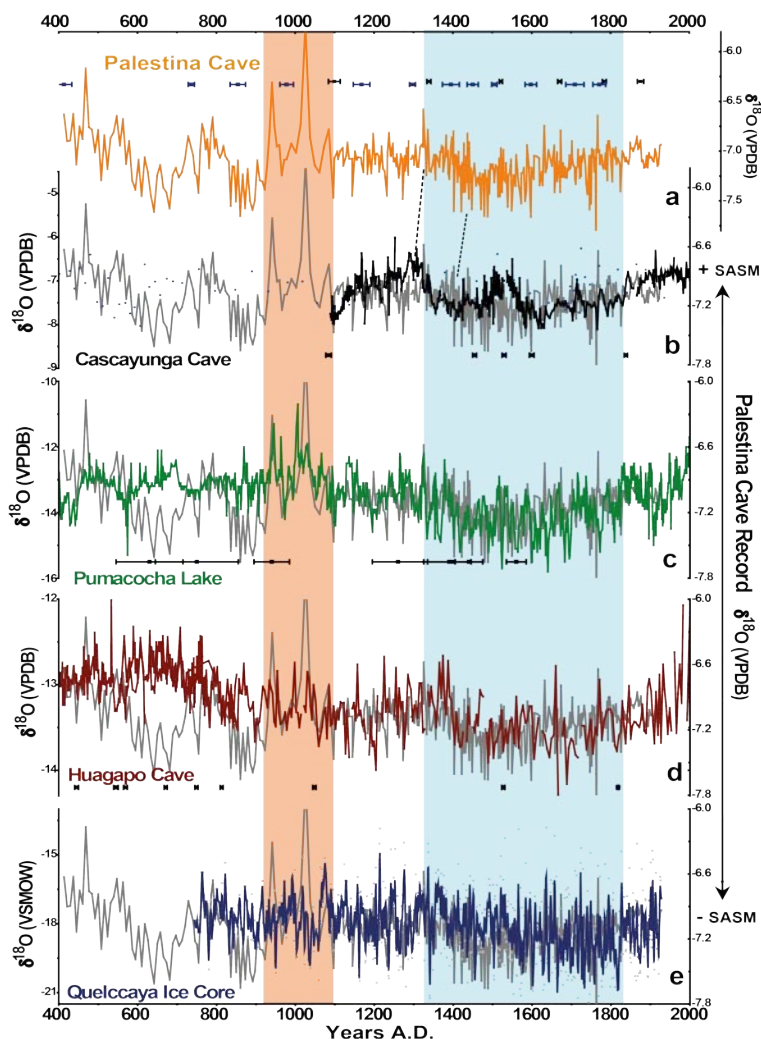


Figure 3. Comparison between Palestina composite record (gray line in the background) and other eastern Andean records with their respective chronological controls and error bars. From top to bottom: (a) Palestina record (this study); (b) Cascayunga record (Reuter et al., 2009); (c) Pumacocha lake record (Bird et al., 2011a); (d) Huagapo cave record (Kanner et al., 2013); (e) Quelccaya Ice Cap (Thompson et al., 1986). Shaded background represents MCA (red) and LIA periods (light blue).

ity of diminished $\delta^{18}\text{O}$ values during the LIA period and timing of the demise of this period is consistent and roughly contemporaneous with the other proxies discussed.

Comparison with other high-resolution proxies of the SASM far from the Andes Cordillera also shows coherent fluctuations of $\delta^{18}\text{O}$ values during the LIA. Over southeastern tropical South America at Cristal cave in Brazil (Fig. 4c), a period of lighter values is observed during the LIA, albeit with some delay in the onset of the minimum values when compared with Andean records (Taylor, 2010; Vuille et al., 2012). Minimum values of $\delta^{18}\text{O}$ in Cristal cave are observed during a relatively short period from AD 1520 to 1736 only. Hence, the start of the LIA in Cristal cave occurs about one hundred years later than the onset of the LIA in the Palestina record and ends a hundred years earlier than the demise of this period in other Andean records.

An interesting finding is revealed by comparisons with speleothem records from northeastern South America, collected at Diva de Moura cave (DV2 record) in the south of the state of Bahia in Brazil (Fig. 4b). During the MCA, defined in this record as the period between AD 890 and 1154, heavier values in $\delta^{18}\text{O}$ are observed, resembling the records from Palestina and Pumacocha. It is quite remarkable to see the similarities between these records, all featuring the same structure of a double peak during the MCA, which is not evident in other proxies in South America. During the LIA, however, variations in the DV2 isotope record are the opposite of what is seen in other records under the influence of the SASM. Moreover, the onset of a trend toward heavier values in the DV2 record occurs around the year AD 1333, which is contemporaneous with the onset of the LIA in many Andean records, supporting the notion of existing telecon-

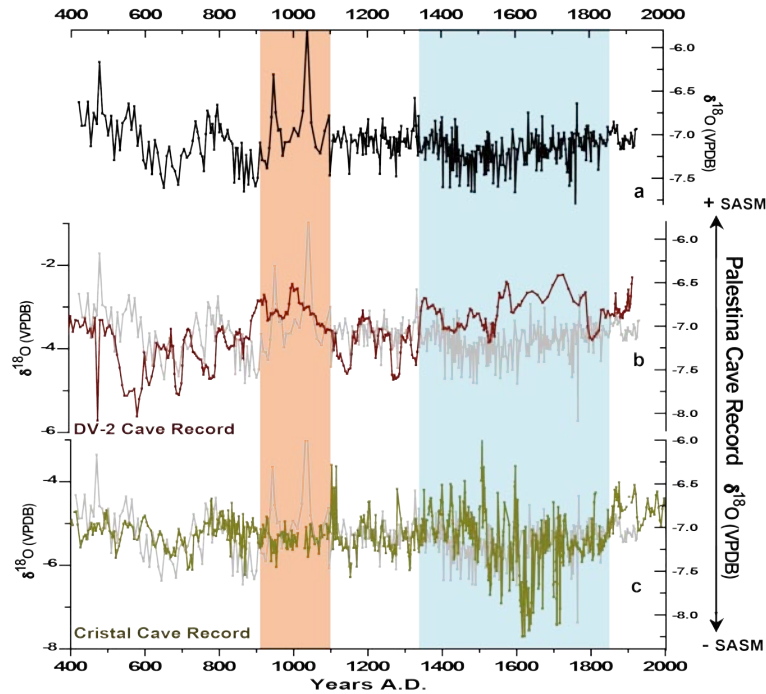


Figure 4. Comparison between Palestina cave $\delta^{18}\text{O}$ record (gray line in the background) and high-resolution proxies of the SAM from non-Andean records: (a) Palestina record (this study), (b) DV-2 cave record (Novello et al., 2012) and (c) Cristal cave record (Taylor, 2010; Vuille et al., 2012).

nections between both regions. At the same time the DV2 record shows similar periodicities affecting summer precipitation as detected in the Palestina record, such as of 76, 65, 40, 22 and 15 years (Novello et al., 2012). These statistically significant periodicities suggest a common large-scale mechanism along the east–west domains of the SAM; probably related to similar climate mechanisms, which are most evident at multidecadal timescales.

4.4 Climatic interpretation

The Palestina oxygen isotope record is interpreted here as a function of SAM activity, consistent with previous studies in the eastern Andes (Bird et al., 2011a; Vuille et al., 2012; Kanner et al., 2013). It shows marked centennial-scale variability spanning the entire record of 1600 years. Two periods with reduced SAM activity stand out from AD 410 to 570 and from AD 720 to 820. Both periods were followed by relatively abrupt changes in enhanced SAM intensity from AD 580 to 720 and between AD 820–920. Higher overall variability in the $\delta^{18}\text{O}$ record from Palestina, when compared with other Andean $\delta^{18}\text{O}$ records, would suggest higher overall precipitation variability at this site during these above periods. It is worth noting that variations in $\delta^{18}\text{O}$ values for these periods are on the same order of magnitude but more sudden than during the MCA and LIA.

The Medieval Climate Anomaly, spanning the period between AD \sim 20 and 1100, shows diminished SAM activ-

ity. A very distinctive double peak structure is observed on decadal timescales, centered at AD \sim 934 and \sim 1039, resulting in the periods of lowest SAM activity in the entire record. Interestingly these features are shared with other records in South America such as Pumacocha lake in the eastern Andes, the DV2 record over northeastern Brazil and peaks of Ti (%) in the Cariaco sediment record, indicative of a displacement of the Intertropical Convergence Zone (ITCZ) to a more northerly position (Haug et al., 2001). The coherence among records from different sites and proxies suggests that a common mechanism triggered these isotopic variations across much of the northern part of the continent. In addition, intense humid events recorded in the Chaac stalagmite on the Yucatan Peninsula are coincident with those peaks (Medina et al., 2010). The sum of all these records suggests that these periods could have been characterized by a reduced moisture influx in to the SAM system during austral summer due to a more northerly position of the ITCZ, and hence more intense rainfall over the tropical Northern Hemisphere during boreal summer. At Palestina cave, the reduced SAM would have lead to less rainout upstream over the Amazon Basin and therefore more enriched $\delta^{18}\text{O}$ values. It is also possible that reduced summer precipitation, and therefore a relatively higher proportion of austral winter precipitation with an enriched signature of $\delta^{18}\text{O}$ could partially explain the magnitude of the two double peaks during the MCA.

Please note the remarks at the end of the manuscript.

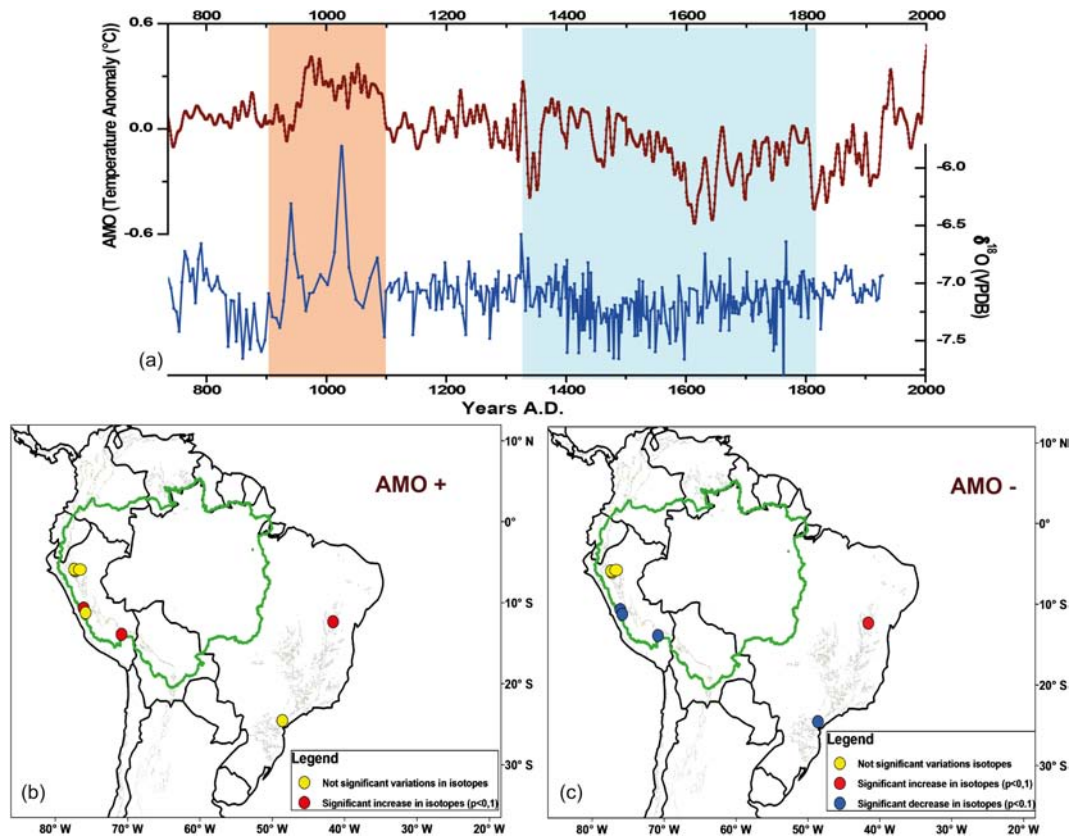


Figure 5. (a) Comparison between the reconstructed AMO index (Mann et al., 2009; red line) and the Palestina record (blue line); (b and c) Departure of $\delta^{18}\text{O}$ from long-term mean during periods when AMO was above the 75th percentile (AMO+, left) and below the 25th percentile (AMO–, right). Significant departures from long-term mean at $p < 0.1$ based on a Student's t test are indicated by red (increase in $\delta^{18}\text{O}$ and blue (decrease in $\delta^{18}\text{O}$) circles. Yellow circles indicate records that do not exhibit any statistically significant changes.

Precipitation over western Amazonia is especially sensitive to changes in tropical Atlantic SSTs, with reduced precipitation when positive SST anomalies are observed in the northern tropical Atlantic [CE1](#) (Espinoza et al., 2011, 2012). There is evidence pointing to unusually warm sea surface temperature anomalies (SSTA) in the North Atlantic sector during the MCA (Keigwin et al., 1996), with characteristics that resemble the positive phase of the AMO (Feng et al., 2008). Indeed, there are indications that the positive phase of the AMO leads to reduced SASM intensity at multidecadal timescales, linked to a northward migration of the ITCZ (Chiessi et al., 2009; Strikis et al., 2011; Bird et al., 2011a; Novello et al., 2012). Periodicities observed in the Palestina cave series highlight a multidecadal influence over the MCA in concordance with the AMO frequency of ~ 65 years, as diagnosed in both model and instrumental data (Knight et al., 2006; Fig. S6). The reconstructed AMO index published by Mann et al. (2009) shows similar characteristics as the Palestina record (Fig. 5a) and also documents a period of persistent positive AMO anomalies during the MCA period, including the same double peak structure, albeit with some lag in the time series. This observation suggests that in north-

ern tropical South America, hydroclimate variability during the MCA might be related to leading expressions [CE2](#) of the North Atlantic Ocean modes. Indeed, previous works have already documented the influence of the Atlantic modes in rainfall distribution and intensity over tropical South America (Reuter et al., 2009; Bird et al., 2011a; Vuille et al., 2012).

Above comparisons between the AMO index (Mann et al., 2009) and the Palestina record revealed strong similarities. The influence of the AMO on South American $\delta^{18}\text{O}$ records is further evaluated by comparing departures in $\delta^{18}\text{O}$ values during positive (+) and negative (–) phases of the AMO (Fig. 5b). Statistically significant negative isotopic anomalies are observed during AMO– over the southern part of tropical South America, which would suggest an enhancement of the SASM during the negative phase of the AMO, affecting predominantly the southern parts of the SASM domain. During AMO+ phases, the isotopic response is spatially less coherent, with a mixture of non-significant and significant positive anomalies scattered across the region. Nonetheless, it is worth noting that there are no significant negative anomalies in any of the records during the AMO+ phase. While most records show a linear response with anomalies of the oppo-

site sign during the two phases of the AMO, this is not the case at all sites. The DV2 record from northeastern South America, in particular, stands out prominently with more enriched values during both positive and negative phase of the AMO. It is worth noting that the Palestina record does not exhibit significant anomalies ($p \leq 0.1$) during either phase of the AMO despite featuring strong similarities with the AMO index. Most likely other factors such as changes in the relative precipitation contribution during different seasons also play a relevant role. This feature is coherent with recent works that documented the role of Pacific and Atlantic oceans on rainfall variability during the austral summer and winter, respectively (Yoon and Zeng, 2012; Espinoza et al., 2011; Marengo et al., 2013).

The transition period from the MCA to the LIA (AD \sim 1100 to 1325) shows mean values of -7.1‰ in $\delta^{18}\text{O}$ characterized by persistent decadal-scale variability. The LIA period itself is characterized by a substantial increase in SASM activity from AD \sim 1325 to 1820, reaching its maximum intensity between AD 1400 and 1593 (-7.6‰ ; Fig. 2). Increased SASM activity during the LIA is synchronous with cold events in the Northern Hemisphere (e.g., Gray et al., 2006; Mann et al., 2009). These cold conditions forced a southward migration of the ITCZ (Haug et al., 2001; Reuter et al., 2009; Bird et al., 2011a; Vuille et al., 2012; Novello et al., 2012) as documented by diminished Ti concentrations in the Cariaco Basin during the LIA (Haug et al., 2001) and a significant decrease in SSTs over the tropical North Atlantic (Black et al., 2007). Since the ITCZ serves as the major moisture source fueling the SASM, an intensification of this system is to be expected from a more southerly position (Vuille et al., 2012), and consistent with the more negative $\delta^{18}\text{O}$ values observed in different proxies across Andean records. The prominent exception to this rule is the DV2 record in northeastern South America, which shows the exact opposite behavior during the LIA with more enriched $\delta^{18}\text{O}$ values suggesting dry conditions. This antiphased behavior, however, might reflect the intensification of the Bolivian high–Nordeste low pressure system, with increased SASM activity and related convective heating over the southwestern portion of the Amazon region (Lenters and Cook, 1997), being balanced by enhanced subsidence and drying over the northeast of the continent (Novello et al., 2012). This mechanism, associated with increased upper level convergence, subsidence and a deficit in summer precipitation over northeastern Brazil during periods of enhanced SASM activity, has been invoked to explain the antiphasing between precipitation in Nordeste rainfall and most of tropical South America on orbital timescales (Cruz et al., 2009). Nevertheless, this mechanism may be nonlinear, and dependent on oceanic boundary conditions (e.g., the state of the tropical Pacific), which could explain why this antiphased behavior occurs during the LIA but not during the MCA.

The Palestina record is consistent with other $\delta^{18}\text{O}$ records along the Andes in the sense that it indicates diminished

SASM activity during the MCA and opposite conditions during the LIA. Both periods were initially recognized in the Northern Hemisphere where the median of reconstructions document mostly warm conditions from about AD 950 to about 1250 (MCA) and colder conditions at about AD 1450–1850 (LIA; IPCC, 2013). In tropical South America, however, the definition of the MCA and LIA events is quite variable between studies and proxies considered, and discrepancies are observed in relation to the intensity and temporal definition of these events (between studies and proxies considered and discrepancies, e.g., Rabatel et al., 2008; Vuille et al., 2012). Indeed, this variability does not seem to be related simply to chronological errors of individual records but may also show a latitudinal migration of the climatic perturbation and its isotopic footprint in and out of this region along the Andes. In order to quantify variations between both events along the Andean region, the average $\delta^{18}\text{O}$ difference between MCA and LIA periods as defined in the Palestina record (AD 900–1100 and 1325–1826) was calculated for all Andean records and divided by their respective standard deviation to make them comparable across proxies.

Larger differences in $\delta^{18}\text{O}$ values between the MCA and the LIA can be observed for the records located in the northern region of the Andes ($< 11^\circ\text{S}$), when compared with proxies located in more southern latitudes (Fig. 6). Taking into account that the $\delta^{18}\text{O}$ signature is sourced from the Atlantic Ocean and that even the altitudinal location of the proxies does not erase the SASM signal (Vuille et al., 2012), it is plausible to suggest that larger MCA–LIA differences at northern locations might be caused by influences other than summer precipitation. In Fig. 6 we also show the seasonal variation coefficient of rainfall (SVC), which is the ratio between the standard deviation of monthly rainfall values (1963–2003) and the mean of monthly rainfall values, considering 756 stations in the Amazon Basin (Espinoza et al., 2009). Indeed, high SVC display a strong rainfall seasonality (i.e., large difference between the wet and dry season), while low SVC values represent weak rainfall seasonality (i.e., small difference between the wet and dry season). The SVCs show reduced seasonality over the northern part of the Andean region. Hence, it is reasonable to assume that during periods of a weakened SASM, the relative contribution of austral winter precipitation linked to heavier isotope values would be enhanced. Such an increased contribution of winter precipitation synchronous with a weakened SASM during the MCA would provide an alternative mechanism that could cause larger differences between both periods in the Andean records, but it might preferentially affect more northern sites.

In order to better understand how variations in the SASM over a broader area of South America relate to the Atlantic Multidecadal Oscillation, cross-wavelet and coherence analyses were developed for both Palestina and DV2 records. In both analyses, results suggest significant periodicities of ~ 64 –80 years as being the most important feature in the time

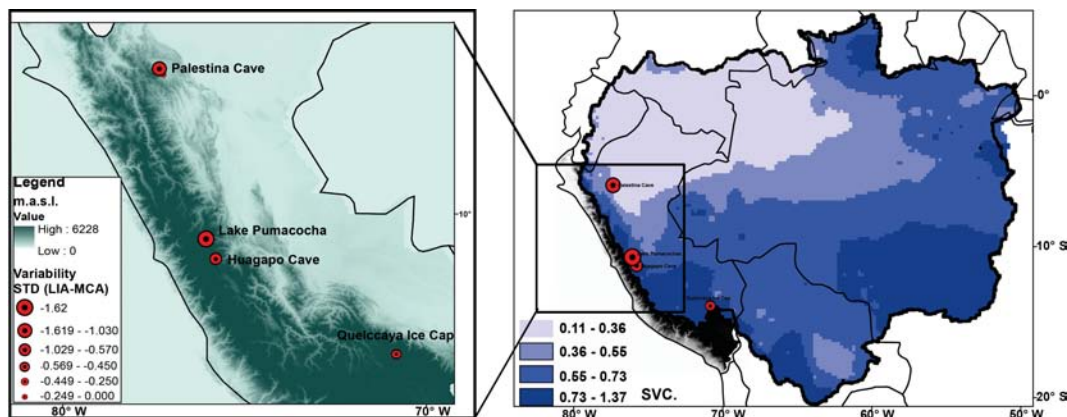


Figure 6. Standardized LIA–MCA difference in the $\delta^{18}\text{O}$ of Andean records plotted with the altitudinal locations of each proxy (left panel); seasonal variability coefficient (SVC) of precipitation calculated for the Amazon Basin (right panel); from Espinoza et al. (2009).

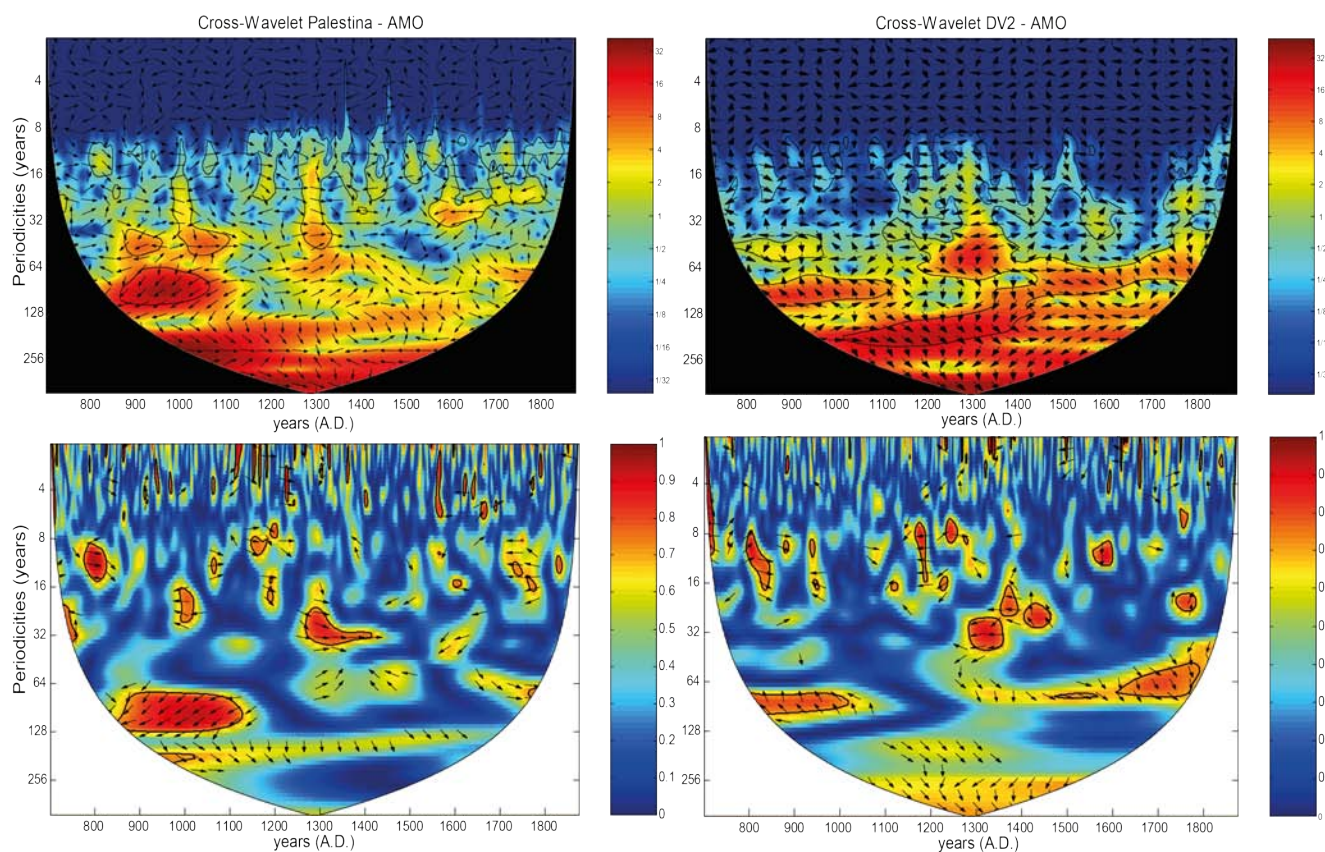


Figure 7. Left panels: cross-wavelets between the AMO index and Palestina record (top) and coherence analysis (bottom) between time series. Right panels: cross-wavelet between DV2 record in Bahia and AMO index (top); coherence analysis is also shown (bottom).

series and with stronger amplitudes during the MCA (Fig. 7). During the LIA, however, even though this low-frequency signal persists, the wavelet analyses suggest that the two regions of the continent were governed by different frequencies (Fig. 7). While in DV2 (NE Brazil) ~ 64 years is the most persistent frequency band, over the eastern Andes higher to

lower frequencies of ~ 25 years and ~ 60 years are superimposed at different periods. Based on these results, we hypothesize that the lower-frequency signals are related to the Atlantic Multidecadal Oscillation, while the slight signal of a ~ 25 -year frequency (between AD 1600 and 1800, in Fig. 7) could be consistent with one of the most energetic signals of

the Pacific Decadal Oscillation. It is hard to disentangle the superimposed influences of the Pacific and Atlantic at different timescales, especially when both oceans trigger distinct modes that may dampen or reinforce one another and lead to nonlinear impacts on rainfall over the South American continent. Nevertheless, based on marine evidence (Sifeddine et al., 2008; Salvattecci et al., 2014), it is possible to assume that during the LIA period, an enhanced role of the Pacific would increase rainfall variability over the eastern Andes.

5 Conclusions

The Palestina record reveals important details of changes in the mean state of the SASM during the past 1600 years and confirms most of the major results from previous paleoclimate reconstructions in the eastern Andes. During the last millennium, SASM activity exhibits departures from the mean state, which are relatively synchronous with major periods of global climate change, recognized as MCA and LIA. The Palestina record adds to the growing network of high-resolution paleoclimate reconstructions for this Andean region and allows replication and thereby confirmation of the veracity of key climate signals from this region, such as the double peak of SASM failure during the peak MCA period. This study highlights that replicating regional climate signals from different sites and using different proxies is absolutely essential for fully understanding past changes in SASM activity, but also in separating climate signals from proxy-specific non-climatic effects. In this sense, the correspondence between records in the Andes and other regions under influence of the SASM is quite remarkable and highlights the ability of $\delta^{18}\text{O}$ to integrate climate signals across large spatial scales affected by common mechanisms such as the SASM.

Comparison between records reveals stronger and more coherent variability during the LIA in the Andean region and over southeastern South America. Moreover, variations in SASM activity between the MCA and the LIA seem to be larger over the northern part of the continent, suggesting a latitudinal dependence of the MCA footprint. Diminished SASM activity and an increase in the relative contribution of winter precipitation would be a plausible mechanism for explaining higher isotopic values during the MCA in the northern tropical sector of the Andes during this period. Since modern records reveal reduced seasonality of precipitation in the northern region of the Amazon Basin, it is reasonable to assume that more positive $\delta^{18}\text{O}$ values could be related to a differential contribution of seasonal precipitation.

In-phase variations between Palestina and DV2 records during the MCA and opposite conditions during the LIA reveal that the influence of oceanic modes over the tropical continent is being modulated in different ways depending on the prevailing boundary conditions. During the MCA the dominant mode of variability is characterized by frequen-

cies around 65 years in both Palestina and DV2, which is consistent with the documented influence of the AMO on SASM precipitation. During the LIA, however, there is no correspondence in the signal between both areas. In fact, decadal variability suggests that other influences may have contributed to decoupling the two regions.

Statistical analyses suggest the influence of the AMO in several South American records, with a generally stronger and spatially more coherent response during the negative phase of the AMO (AMO⁻). This analysis also highlights that the AMO influence is not always linear, as shown, for example, for the case of the DV2 record, which exhibits significant positive departures during both phases of the AMO. Nevertheless, a stronger focus on studying multidecadal variability of the SASM during both recent and past periods seems warranted in order to enhance our understanding of this unique monsoon system and to better prepare society for future changes associated with anthropogenic climate change.

The Supplement related to this article is available online at doi:10.5194/cp-10-1-2014-supplement.

Acknowledgements. We thank Luis Mancini and Ana Carolina Miranda for their support during the stable isotope data acquisition at the Universidade de Brasília and Osmar Antunes for his support at Universidade de São Paulo. We also thank Augusto Auler, Daniel Menin and the Espeleo Club Andino (ECA Perú) for their support during the field work. This work was undertaken as part of the the PALEOTRACES project (IRD-UFF-UANTOF), HYBAM Project (IRD) and PRIMO cooperative project (CNPq-IRD), and supported by the Fundação de Amparo a Pesquisa do Estado de Rio de Janeiro, Brazil (FAPERJ grant E-26/100.377/2012), Fundação de Amparo a Pesquisa do Estado de São Paulo, Brazil (FAPESP grants 2011/39450394 to F. W. Cruz and 2012/50260-6 and University of São Paulo through INCLINE research group) and also by grants 2013CB955902, CNSF 41230524, US NSF grants 0502535 and 3961103404 to L. Edwards and H. Cheng and NSF grants 1003690 and 1303828 to M. Vuille. We are also grateful to the anonymous reviewers, whose comments helped to significantly improve the manuscript. We wish to recognize their effort and time spent to help put this record into the regional paleoclimate framework of tropical South America.

Edited by: E. Zorita

References

- Bird, B. W., Abbott, M. B., Vuille, M., Rodbell, D. T., Stansell, N. D., and Rosenmeier, M. F.: A 2300-year-long annually resolved record of the South American summer monsoon from the Peruvian Andes, *P. Natl. Acad. Sci.*, 108, 8583–8588, 2011a.

- Bird, B. W., Abbott, M. B., Rodbell, D. T., and Vuille, M.: Holocene tropical South American hydroclimate revealed from a decadal resolved lake sediment $\delta^{18}\text{O}$ record, *Earth Planet. Sc. Lett.*, 310, 192–202, 2011b.
- Black, D. E., Abahazi, M. A., Thunell, R. C., Kaplan, A., Tappa, E. J., and Peterson, L. C.: An 8-century tropical Atlantic SST record from the Cariaco Basin: Baseline variability, twentieth-century warming, and Atlantic hurricane frequency, *Paleoceanography*, 22, PA4204, doi:10.1029/2007PA001427, 2007.
- Cheng, H., Edwards, L. R., Shen, C.-C., Polyak, V. J., Asmerom, Y., Woodhead, J., Hellstrom, J., Wang, Y., Kong, X., Spötl, C., Wang, X., and Alexander Jr., E. C.: Improvements in ^{230}Th dating, ^{230}Th and ^{234}U half-life values, and U–Th isotopic measurements by multi-collector inductively coupled plasma mass spectrometry, *Earth Planet. Sci. Lett.*, 371–372, 82–91, doi:10.1016/j.epsl.2013.04.006, 2013.
- Chiessi, C., Mulitza, S., Paetzold, J., Wefer, G., and Marengo, J.: Possible impact of the Atlantic Multidecadal Oscillation on the South American summer monsoon, *Geophys. Res. Lett.*, 36, L21707, doi:10.1029/2009GL039914, 2009.
- Cobb, K. M., Charles, C. D., Cheng, H., and Edwards, R. L.: El Niño/Southern Oscillation and tropical Pacific climate during the last millennium, *Nature*, 424, 271–276, 2003. [TS5](#)
- Conroy, J. L., Overpeck, J. T., Cole, J. E., Shanahan, T. M., and Steinitz-Kannan, M.: Holocene changes in eastern tropical Pacific climate inferred from a Galápagos lake sediment record, *Quaternary Sci. Rev.*, 27, 1166–1180, 2008. [TS6](#)
- Cruz, F. W., Vuille, M., Burns, S. J., Wang, X., Cheng, H., Werner, M., Lawrence Edwards, R., Karmann, I., Auler, A. S., and Nguyen, H.: Orbitally driven east–west antiphasing of South American precipitation, *Nat. Geosci.*, 2, 210–214, doi:10.1038/ngeo444, 2009.
- Edwards, R. L., Chen, J. H., and Wasserburg, G. J.: ^{238}U – ^{234}U – ^{230}Th – ^{232}Th systematics and the precise measurement of time over the past 500 000 years, *Earth Planet. Sc. Lett.*, 81, 175–192, 1987.
- Espinoza, J. C., Ronchail, J., Guyot, J. L., Cocheneau, G., Filizola, N., Lavado, W., de Oliveira, E., Pombosa, R., and Vauchel, P.: Spatio–Temporal rainfall variability in the Amazon Basin Countries (Brazil, Peru, Bolivia, Colombia and Ecuador), *Int. J. Climatol.*, 29, 1574–1594, 2009.
- Espinoza, J. C., Ronchail, J., Guyot, J. L., Junquas, C., Vauchel, P., Lavado, W. S., Drapeau, G., and Pombosa, R.: Climate variability and extremes drought in the upper Solimões River (Western Amazon Basin): Understanding the exceptional 2010 drought, *Geophys. Res. Lett.*, 38, L13406, doi:10.1029/2011GL047862, 2011.
- Espinoza, J. C., Ronchail, J., Guyot, J. L., Junquas, C., Drapeau, G., Martinez, J. M., Santini W., Vauchel, P., Lavado, W., Ordoñez, J., and Espinoza, R.: From drought to flooding: understanding the abrupt 2010–2011 hydrological annual cycle in the Amazonas River and tributaries, *Environ. Res. Lett.*, 7, 024008, doi:10.1088/1748-9326/7/2/024008, 2012.
- Espinoza, J. C., Ronchail, J., Frappart, F., Lavado, W., Santini, W., and Guyot, J. L.: The Major Floods in the Amazonas River and Tributaries (Western Amazon Basin) during the 1970–2012 Period: A Focus on the 2012 Flood, *J. Hydrometeorol.*, 14, 1000–1008, 2013.
- Feng, S., Oglesby, R. J., Rowe, C., Loope, D., and Hu, Q.: Atlantic and Pacific SST influences on Medieval drought in North America simulated by the Community Atmospheric Model, *J. Geophys. Res.*, 113, D11101, doi:10.1029/2007JD009347, 2008.
- Gao, C., Robock, A., and Ammann, C.: Volcanic forcing of climate over the past 1500 years: an improved ice-core-based index for climate models, *J. Geophys. Res.*, 113, D23111, doi:10.1029/2008JD010239, 2008. [TS7](#)
- Garreaud, R., Vuille, M., and Clement, A.: The climate of the Altiplano: Observed current conditions and mechanisms of past changes, *Palaeogeogr. Palaeoclimatol.*, 194, 5–22, 2003.
- Garreaud, R. D., Vuille, M., Compagnucci, R., and Marengo, J.: Present-day South American climate, *Palaeogeogr. Palaeoclimatol.*, 281, 180–195, 2009.
- Gonzalez-Rouco, F. J., Fernandez-Donado, L., Raible, C. C., Barriopedro, D., Luterbacher, J., Jungclauss, J. H., Swingedouw, D., Servonnat, J., Zorita, E., Wagner, S., and Ammann, C. M.: Medieval Climate Anomaly to Little Ice Age transition as simulated by current climate models, *PAGES news* 19, 7–8, 2011. [TS8](#)
- Graham, N. E., Ammann, C. M., Fleitmann, D., Cobb, K. M., and Luterbacher, J.: Support for global climate reorganization during the “Medieval Climate Anomaly”, *Clim. Dynam.*, 37, 1217–1245, doi:10.1007/s00382-010-0914-z, 2010.
- Gray, S. T., Graumlich, L. J., Betancourt, J. L., and Pederson, G. T.: A tree-ring based reconstruction of the Atlantic Multidecadal Oscillation since 1567 A.D., *Geophys. Res. Lett.*, 31, L12205, doi:10.1029/2004GL019932, 2004. [TS9](#)
- Grimm, A. M.: Interannual climate variability in South America? Impacts on seasonal precipitation, extreme events, and possible effects of climate change, *Stoch. Env. Res. Risk A.*, 25, 537–554, doi:10.1007/s00477-010-0420-1, 2010.
- Grimm, A. M. and Zilli, M. T.: Interannual Variability and Seasonal Evolution of Summer Monsoon Rainfall in South America, *J. Climate*, 22, 2257–2275, 2009.
- Grinsted, A., Jevrejeva, S., and Moore, J.: Application of the cross wavelet transform and wavelet coherence to geophysical time series, *Nonlinear Proc. Geoph.*, 11, 561–566, 2004.
- Gutiérrez, D., Sifeddine, A., Field, D. B., Ortlieb, L., Vargas, G., Chávez, F. P., Velasco, F., Ferreira, V., Tapia, P., Salvatelli, R., Boucher, H., Morales, M. C., Valdés, J., Reyss, J.-L., Campusano, A., Boussafir, M., Mandeng-Yogo, M., García, M., and Baumgartner, T.: Rapid reorganization in ocean biogeochemistry off Peru towards the end of the Little Ice Age, *Biogeosciences*, 6, 835–848, doi:10.5194/bg-6-835-2009, 2009. [TS10](#)
- Ham, Y.-G., Kug, J.-S., Park, J.-Y., and Jin, F.-F.: Sea surface temperature in the north tropical Atlantic as a trigger for El Niño/Southern Oscillation events, *Nat. Geosci.*, 6, 112–116, doi:10.1038/ngeo1686, 2013. [TS11](#)
- Haug, G. H., Hughen, K., Sigman, D. M., Peterson, L. C., and Röhl, U.: Southward migration of the intertropical convergence zone through the Holocene, *Science*, 293, 1304–1308, 2001.
- IPCC 2013: Masson-Delmotte, V., Schulz, M., Abe-Ouchi, A., Beer, J., Ganopolski, A., González Rouco, J. F., Jansen, E., Lambbeck, K., Luterbacher, J., Naish, T., Osborn, T., Otto-Bliessner, B., Quinn, T., Ramesh, R., Rojas, M., Shao, X., and Timmermann, A.: Information from Paleoclimate Archives, in: *Climate Change 2013: The Physical Science Basis. Contribution of Working Group I to the Fifth Assessment Report of the Intergovernmental Panel on Climate Change*, edited by: Stocker, T. F., Qin, D.,

- Plattner, G.-K., Tignor, M., Allen, S. K., Boschung, J., Nauels, A., Xia, Y., Bex, V., and Midgley, P. M.: Cambridge University Press, Cambridge, United Kingdom and New York, NY, USA, 2013.
- Jomelli, V., Favier, V., Rabatel, A., Brunstein, D., Hoffmann, G., and Francou, B.: Fluctuations of glaciers in the tropical Andes over the last millennium and palaeoclimatic implications: A review, *Palaeogeogr. Palaeoclimatol.*, 281, 269–282, doi:10.1016/j.palaeo.2008.10.033, 2009.
- Kanner, L. C., Burns, S. J., Cheng, H., Edwards, R. L., and Vuille, M.: High-resolution variability of the South American summer monsoon over the last seven millennia: insights from a speleothem record from the central Peruvian Andes, *Quaternary Sci. Rev.*, 75, 1–10, doi:10.1016/j.quascirev.2013.05.008, 2013.
- Keigwin, L.: The Little Ice Age and Medieval Warm Period in the Sargasso Sea, *Science*, 274, 1504–1508, 1996.
- Knight, J. R., Folland, C. K., and Scaife, A. A.: Climate impacts of the Atlantic Multidecadal Oscillation, *Geophys. Res. Lett.*, 33, L17706, doi:10.1029/2006GL026242, 2006.
- Lavado, W., Labat, D., Ronchail, J., Espinoza, J. C., and Guyot, J. L.: Trends in rainfall and temperature in the Peruvian Amazon – Andes basin over the last 40 years (1965–2007), *Hydrological Processes*, [TS12](#), doi:10.1002/hyp.9418, 2012.
- Lenters, J. D. and Cook, K. H.: On the origin of the Bolivian high and related circulation features of the South American climate, *J. Atmos. Sci.*, 54, 656–678, 1997.
- Mann, M. E.: Little Ice Age, *Encyclopedia of Global Environmental Change*, ISBN 0-471-97796-9, 1, 504–509, 2002.
- Mann, M. E., Zhang, Z., Rutherford, S., Bradley, R. S., Hughes, M. K., Shindell, D., Ammann, C., Faluvegi, G., and Ni, F.: Global signatures and dynamical origins of the Little Ice Age and Medieval Climate Anomaly, *Science*, 326, 1256–1260, 2009.
- Mantua, N. and Hare, S.: The Pacific Decadal Oscillation (review), *J. Oceanogr.*, 58, 35–44, 2002. [TS13](#)
- Mantua, N. J., Hare, S. R., Zhang, Y., Wallace, J. M., and Francis, R. C.: A Pacific interdecadal climate oscillation with impacts on salmon production, *B. Am. Meteorol. Soc.*, 78, 1069–1079, 1997. [TS14](#)
- Marengo, J. A. and Nobre, C. A.: General characteristics and variability of climate in the Amazon basin and its links to the global climate system. *The Biogeochemistry of the Amazon Basin*, Oxford University Press, Oxford, UK, 17–41, 2001.
- Marengo, J. A., Nobre, C. A., Tomasella, J., Oyama, M. D., De Oliveira, G. S., De Oliveira, R., Camargo, H., Alves, L. M., and Brown, I. F.: The drought of Amazonia in 2005, *J. Climate*, 21, 495–516, 2008.
- Marengo, J. A., Liebmann, B., Grimm, A. M., Misra, V., Silva Dias, P. L., Cavalcanti, I. F. A., Carvalho, L. M. V., Berbery, E. H., Ambrizzi, T., Vera, C. S., Saulo, A. C., Nogueira-Paegle, J., Zipser, E., Seth, A., and Alves, L. M.: Recent developments on the South American monsoon system, *Int. J. Climatol.*, 32, 1–21, 2012.
- Medina-Elizalde, M., Burns, S. J., Lea, D. W., Asmerom, Y., Von Gunten, L., Polyak, V., Vuille, M., and Karmalkar, A.: High resolution stalagmite climate record from the Yucatán Peninsula spanning the Maya terminal classic period, *Earth Planet. Sc. Lett.*, 298, 255–262, 2010.
- Mignot, J., Khodri, M., Frankignoul, C., and Servonnat, J.: Volcanic impact on the Atlantic Ocean over the last millennium, *Clim. Past*, 7, 1439–1455, doi:10.5194/cp-7-1439-2011, 2011. [TS15](#)
- Moy, C. M., Seltzer, G. O., Rodbell, D. T., and Anderson, D. M.: Variability of El Niño/Southern Oscillation activity at millennial timescales during the Holocene epoch, *Nature*, 420, 162–165, 2002. [TS16](#)
- Newton, A., Thunell, R., and Stott, L.: Climate and hydrographic variability in the Indo-Pacific Warm Pool during the last millennium, *Geophys. Res. Lett.*, 33, L19710, doi:10.1029/2006GL027234, 2006. [TS17](#)
- Nogués-Paegle, J. and Mo, K.: Alternating wet and dry conditions over South America during summer, *Mon. Weather Rev.*, 125, 279–291, 1997. [TS18](#)
- Nogués-Paegle, J. N. and Mo, K. C.: Linkages between summer rainfall variability over South America and sea surface temperature anomalies, *J. Climate*, 15, 1389–1407, 2002.
- Novello, V. F., Cruz, F. W., Karmann, I., Burns, S. J., Strikis, N. M., Vuille, M., Cheng, H., Edwards, L. R., Santos, V. R., Frigo, E., and Barreto, E. A. S.: Multidecadal climate variability in Brazil's Nordeste during the last 3000 years based on speleothem isotope records, *Geophys. Res. Lett.*, 39, L23706, doi:10.1029/2012GL053936, 2012.
- Oliveira, S. M., Marques Gouveia, S. S. E., Pessenda, L., Favaro, C. R., and Teixeira, D. I.: Lacustrine sediments provide geochemical evidence of environmental change during the last millennium in southeastern Brazil, *Chemie der Erde*, 69, 395–405, 2009.
- Oppo, D. W., Rosenthal, Y., and Linsley, B. K.: 2000-year-long temperature and hydrology reconstructions from the Indo-Pacific warm pool, *Nature*, 460, 1113–1116, 2009. [TS19](#)
- PAGES-2k-Consortium, Continental-scale temperature variability during the past two millennia, *Nat. Geosci.*, 6, 339–346, 2013. [TS20](#)
- Palastanga, V., van der Schrier, G., Weber, S. L., Kleinen, T., Briffa, K. R., and Osborn, T. J.: Atmosphere and ocean dynamics: contributors to the European Little Ice Age?, *Clim. Dynam.*, 36, 973–987, 2011. [TS21](#)
- Parsons, L. A., Yin, J., Overpeck, J. T., Stouffer, R. J., and Malyshev, S.: Influence of the Atlantic Meridional Overturning Circulation on the monsoon rainfall and carbon balance of the American tropics, *Geophys. Res. Lett.*, 41, 146–151, doi:10.1002/2013GL058454, 2014.
- Rabatel, A., Francou, B., Jomelli, V., Naveau, P., and Grancher, D.: A chronology of the Little Ice Age in the tropical Andes of Bolivia (16° S) and its implications for climate reconstruction, *Quaternary Res.*, 70, 198–212, doi:10.1016/j.yqres.2008.02.012, 2008.
- Reuter, J., Stott, L., Khider, D., Sinha, A., Cheng, H., and Edwards, R. L.: A new perspective on the hydroclimate variability in northern South America during the Little Ice Age, *Geophys. Res. Lett.*, 36, L21706, doi:10.1029/2009GL041051, 2009.
- Robertson, A. W. and Mechoso, C. R.: Interannual and Decadal Cycles in River Flows of Southeastern South America, *J. Climate*, 11, 2570–2581, 1998. [TS22](#)
- Ronchail, J., Cochonneau, G., Molinier, M., Guyot, J. L., Gorette de Miranda Chaves, A., Guimarães, V., and de Oliveira, E.: Rainfall Variability in the Amazon Basin and SSTs in the tropical Pacific and Atlantic oceans, *Int. J. Climatol.*, 22, 1663–1686, 2002.
- Rozanski, K., Araguás-Araguás, L., and Gonfiantini, R.: Relation between long-term trends of oxygen-18 isotope composition of precipitation and climate, *Science*, 258, 981–985, 1992.

- Sachs, J. P., Sachse, D., Smittenberg, R. H., Zhang, Z., Battisti, D. S., and Golubic, S.: Southward movement of the Pacific intertropical convergence zone AD 1400–1850, *Nat. Geosci.*, 2, 519–525, doi:10.1038/ngeo554, 2009.
- Salvatteci, R., Gutiérrez, D., Field, D., Sifeddine, A., Ortlieb, L., Bouloubassi, I., Boussafir, M., Boucher, H., and Cetin, F.: The response of the Peruvian Upwelling Ecosystem to centennial-scale global change during the last two millennia, *Clim. Past*, 10, 715–731, doi:10.5194/cp-10-715-2014, 2014.
- Seth, A., Rojas, M., and Rauscher, S. A.: CMIP3 projected changes in the annual cycle of the South American monsoon, *Climatic Change*, 98, 331–357, 2010.
- Sifeddine, A., Gutiérrez, D., Ortlieb, L., Boucher, H., Velazco, F., Field, D., Vargas, G., Boussafir, M., Salvatteci, R., Ferreira, V., García, M., Valdés, J., Caquineau, S., Mandeng Yogo, M., Cetin, F., Solis, J., Soler, P., and Baumgartner, T.: Laminated sediments from the central Peruvian continental slope: A 500 year record of upwelling system productivity, terrestrial runoff and redox conditions, *Prog. Oceanogr.*, 79, 190–197, 2008.
- Silva, G. A. M., Ambrizzi, T., and Marengo, J. A.: Observational evidences on the modulation of the South American Low Level Jet east of the Andes according the ENSO variability, *Ann. Geophys.*, 27, 645–657, doi:10.5194/angeo-27-645-2009, 2009.
- Strikis, N. M., Cruz Jr., F. W., Cheng, H., Karmann, I., Edwards, R. L., Vuille, M., Wang, X., de Paula, M. S., Novello, V. F., and Auler, A. S.: Abrupt variations in South American monsoon rainfall during the Holocene based on a speleothem record from central-eastern Brazil, *Geology*, 39, 1075–1078, 2011.
- Taylor, B. L.: A speleothems-based high resolution reconstruction of climate in southeastern Brazil over the past 4100 years, M. S. thesis, University of Massachusetts, Massachusetts, USA, 2010.
- Thompson, L. G., Mosley-Thompson, E., Bolzan, J. F., and Koci, B. R.: A 1500-year record of tropical precipitation in ice cores from the Quelccaya ice cap, Peru, *Science*, 229, 971–973, 1985.
- Thompson, L. G., Mosley-Thompson, E., Dansgaard, W., and Grootes, P. M.: The Little Ice Age as recorded in the stratigraphy of the tropical Quelccaya Ice Cap, *Science*, 234, 361–364, 1986.
- Thompson, L. G., Mosley-Thompson, E., Davis, M. E., Zagorodnov, V. S., Howat, I. M., Mikhalenko, V. N., and Lin, P.-N.: Annually resolved ice core records of tropical climate variability over the past ~ 1800 years, *Science*, 340, 945–50, doi:10.1126/science.1234210, 2013.
- Torrence, C. and Compo, G. P.: A practical guide to wavelet analysis, *B. Am. Meteorol. Soc.*, 79, 61–78, 1998.
- Trouet, V. and Baker, A.: Reconstructing climate dynamics over the past Millennium, *Eos*, 90, 283–284, 2009. [TS23](#)
- Trouet, V., Esper, J., Graham, N. E., Baker, A., Scourse, J. D., and Frank, D. C.: Persistent positive North Atlantic oscillation mode dominated the Medieval Climate Anomaly, *Science*, 324, 78–80, 2009. [TS24](#)
- Trouet, V., Scourse, J. D., and Raible, C. C.: North Atlantic storminess and Atlantic Meridional Overturning Circulation during the last Millennium: Reconciling contradictory proxy records of NAO variability, *Global Planet. Change*, 84–85, 48–55, 2012. [TS25](#)
- Van Breukelen, M., Vonhof, H., Hellstrom, J., Wester, W., and Kroon, D.: Fossil dripwater in stalagmites reveals Holocene temperature and rainfall variation in Amazonia, *Earth Planet. Sc. Lett.*, 275, 54–60, 2008.
- Vera, C. S., Higgins, W., Amador, J., Ambrizzi, T., Garreaud, R., Gochis, D., Gutzler, D., Lettenmaier, D., Marengo, J. A., Mechoso, C. R., Nogues-Paegle, J., Silva Dias, P. L., and Zhang, C.: Toward a Unified View of the American Monsoon Systems, *J. Climate*, 19, 4977–5000, 2006. [TS26](#)
- Vimeux, F., Gallaire, R., Bony, S., Hoffmann, G., and Chiang, J. C. H.: What are the climate controls on δD in precipitation in the Zongo Valley (Bolivia)? Implications for the Illimani ice core interpretation, *Earth Planet. Sc. Lett.*, 240, 205–220, 2005.
- Vuille, M. and Werner, M.: Stable isotopes in precipitation recording South American summer monsoon and ENSO variability – observations and model results, *Clim. Dynam.*, 25, 401–413, doi:10.1007/s00382-005-0049-9, 2005
- Vuille, M., Bradley, R. S., Werner, M., Healy, R., and Keimig, F.: Modeling $\delta^{18}O$ in precipitation over the tropical Americas: 1. Interannual variability and climatic controls, *J. Geophys. Res.*, 108, 4174, doi:10.1029/2001JD002038, 2003. [TS27](#)
- Vuille, M., Burns, S. J., Taylor, B. L., Cruz, F. W., Bird, B. W., Abbott, M. B., Kanner, L. C., Cheng, H., and Novello, V. F.: A review of the South American monsoon history as recorded in stable isotopic proxies over the past two millennia, *Clim. Past*, 8, 1309–1321, doi:10.5194/cp-8-1309-2012, 2012.
- Wunsch, C.: The interpretation of short climate records, with comments on the North Atlantic and Southern Oscillations, *B. Am. Meteorol. Soc.*, 80, 245–255, 1999. [TS28](#)
- Yoon, J.-H. and Zeng, N.: An Atlantic influence on Amazon rainfall, *Clim. Dynam.*, 34, 249–264, doi:10.1007/s00382-009-0551-6, 2010.
- Zhong, Y., Miller, G. H., Otto-Bliesner, B. L., Holland, M. M., Bailey, D. A., Schneider, D. P., and Geirsdottir, A.: Centennial-scale climate change from decadal-paced explosive volcanism: a coupled sea ice-ocean mechanism, *Clim. Dynam.*, 37, 2373–2387, doi:10.1007/s00382-010-0967-z, 2010. [TS29](#)

Remarks from the language copy-editor

- CE1** Elsewhere you have mentioned the tropical North Atlantic. Are these two the same? Please maintain consistency throughout the manuscript.
- CE2** Is there another way to explain this? The use of “expressions” may be confusing.

Remarks from the typesetter

- TS1** Please provide city.
- TS2** Please define if it is 2011a or b.
- TS3** Reference is not mentioned in the reference list.
- TS4** Reference is not mentioned in the reference list.
- TS5** Reference is not cited in the text.
- TS6** Reference is not cited in the text.
- TS7** Reference is not cited in the text.
- TS8** Reference is not cited in the text.
- TS9** Please check doi.
- TS10** Reference is not cited in the text.
- TS11** Reference is not cited in the text.
- TS12** Please provide volume and page range.
- TS13** Reference is not cited in the text.
- TS14** Reference is not cited in the text.
- TS15** Reference is not cited in the text.
- TS16** Reference is not cited in the text.
- TS17** Reference is not cited in the text.
- TS18** Reference is not cited in the text.
- TS19** Reference is not cited in the text.
- TS20** Reference is not cited in the text.
- TS21** Reference is not cited in the text.
- TS22** Reference is not cited in the text.
- TS23** Reference is not cited in the text.
- TS24** Reference is not cited in the text.
- TS25** Reference is not cited in the text.
- TS26** Reference is not cited in the text.
- TS27** Reference is not cited in the text.
- TS28** Reference is not cited in the text.
- TS29** Reference is not cited in the text.